

Hysteretic behavior of the vortex lattice at the onset of the second peak for the $\text{HgBa}_2\text{CuO}_{4+\delta}$ superconductor

D. Stamopoulos and M. Pissas

Institute of Materials Science, NCSR "Demokritos," 153-10, Aghia Paraskevi, Athens, Greece

(Received 19 October 2001; revised manuscript received 22 January 2002; published 27 March 2002)

By means of local Hall probe ac and dc permeability measurements, we investigate the phase diagram of vortex matter for the $\text{HgBa}_2\text{CuO}_{4+\delta}$ superconductor in the regime near critical temperature. The second peak line H_{sp} , in contrast to what is usually assumed, does not terminate at the critical temperature. Our local ac permeability measurements reveal a pronounced hysteretic behavior and thermomagnetic history effects near the onset of the second peak, giving evidence of a phase transition of vortex matter from an ordered quasilattice state to a disordered glass.

DOI: 10.1103/PhysRevB.65.134524

PACS number(s): 74.60.Ge, 74.72.Gr, 74.60.Jg

It is remarkable that after a decade of experimental and theoretical efforts^{1,2} the vortex matter phase diagram of high- T_c superconductors under the presence of random point disorder is far from being completely elucidated. Soon after the discovery of high- T_c superconductors, it was proposed that point disorder should transform the ideal vortex lattice to a glassy state. This state is characterized by energy barriers $U(j)$ that diverge in the limit of small applied currents j . Two main phenomenological theories have been proposed to describe this glassy phase. The first theory is based on the gauge glass model, and assumes a complete destruction of the ideal vortex lattice.³ The second theory retains the elastic lattice structure at small scales.¹ Although different in nature, both theories agree that point disorder dictates the appearance of dislocations, producing a glassy low-temperature phase where the perfect flux lattice is completely distorted at large length scales.

Recently, theoretical proposals provided a description valid at all scales, demonstrating that while disorder produces an algebraic growth of displacements at short length scales, periodicity takes over at large scales, resulting in a decay of translational order at most algebraic.⁴⁻¹¹ One striking prediction is, thus, the existence of a glass phase that should exhibit Bragg diffraction peaks in neutron-scattering measurements.¹² This vortex state is the so-called Bragg glass.⁴ When the field is increased the Bragg glass should undergo a transition into another phase, which could be a pinned liquid or another vortex glass.⁴ Such a field-driven transition corresponds to the destruction of the Bragg glass by a proliferation of topological defects, upon raising the field, which is equivalent to *increasing the effective disorder*, which favors dislocations. Today, the nature of the transition between the two phases, and the exact position of this phase boundary on the phase diagram (H, T), are not well understood.

Between the elastic quasilattice and the highly disordered vortex glass there should be a distinct difference, concerning the dependence of magnetization measurements on the thermomagnetic history, similar to what was observed in other disordered systems. Such history effects have been observed in transport and magnetic measurements for the low- T_c superconductors, in the region of the conventional peak effect

close to the upper critical field line.¹³⁻¹⁸ It was suggested that in this regime plastic deformations occur in the solid, leading to a dependence of the hysteretic response on the past history of the superconductor.

The situation is rather different for the case of high- T_c superconductors. The effect of a second peak (or fishtail peak) on the magnetization loops is still of unknown origin, while the simultaneous appearance of double-peak structures¹⁹⁻²⁵ makes the interpretation more complicated. Today there is experimental evidence for the existence of a crossover point H'_{sp} , that lies between the second peak H_{sp} and its onset point H_{onset} , where the dynamic behavior of the vortex solid changes drastically from elastic (below H'_{sp}) to plastic (above H'_{sp}).²⁶⁻²⁹ Furthermore, several experimental works presented evidence that in clean $\text{YBa}_2\text{Cu}_3\text{Cu}_{7-\delta}$ and $\text{Bi}_2\text{Sr}_2\text{CaCu}_2\text{O}_{8+\delta}$ crystals the boundary between the Bragg and vortex glass states is in close proximity to the onset H_{onset} of the second magnetization peak.³⁰⁻³² In addition, dc magnetization measurements in pure high-quality single crystals of $\text{YBa}_2\text{Cu}_3\text{Cu}_{7-\delta}$ revealed the existence of a kink (near the onset of the fishtail peak) in the magnetization loops,³³⁻³⁵ and a pronounced history dependence^{36,37,22,34} in the regime between the fishtail peak and its onset field.

In this paper we report on local dc and ac permeability measurements for the $\text{HgBa}_2\text{CuO}_{4+\delta}$ superconductor, which displays an intermediate anisotropy in comparison to that of $\text{YBa}_2\text{Cu}_3\text{Cu}_{7-\delta}$ and $\text{Bi}_2\text{Sr}_2\text{CaCu}_2\text{O}_{8+\delta}$. With the present study we hope to elucidate the phase diagram of vortex matter under the presence of point disorder, near the critical temperature. The limited range in the dc field ($H_{dc} < 1000$ Oe) that can be applied in our local Hall magnetometer enforced us to study a disordered single crystal that exhibits a second peak line that terminates in the low-field regime, close to the critical temperature.²⁵ In our local ac permeability curves we observed a hysteretic behavior in the region between the onset and the second peak (the fishtail peak). Partial loop measurements revealed a pronounced dependence of the ac permeability on the thermomagnetic history, in the regime under discussion. In addition, this particular single crystal, except for the fishtail peak, displays a third peak near the irreversibility line which resembles the conventional peak effect.

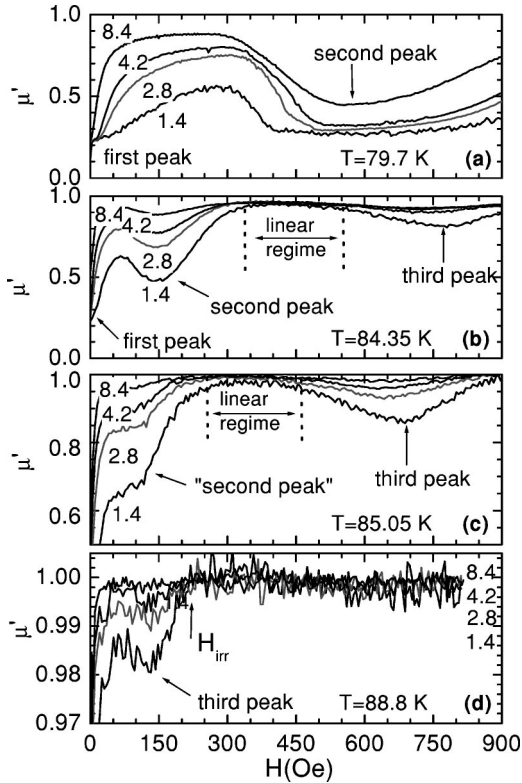


FIG. 1. Real part $\mu' = B'/H_0$ of the local fundamental ac permeability as a function of the dc magnetic field at $T = 77.8$ – 89.9 K for various ac fields, $H_0 = 1.4, 2.8, 4.2,$ and 8.4 Oe ($\mathbf{H}_{dc}, \mathbf{H}_{ac} \parallel c$).

The single-crystal growth procedure was reported elsewhere.^{38,39} Our single crystal displays a value of $T_c = 89.9$ K, with a transition width of 1.5 K and dimensions $600 \times 900 \times 15 \mu\text{m}^3$. For our local magnetic induction measurements we used a $\text{Ga}_x\text{As}_{1-x}\text{In}$ Hall sensor with an active area of $50 \times 50 \mu\text{m}^2$. The single crystal was placed directly on top of the active area of the Hall sensor. The local magnetic induction at the surface of the crystal was measured using an ac magnetic field [$H_{ac} = H_0 \sin(2\pi ft)$, $f = 10$ Hz], under the presence of a dc magnetic field ($\mathbf{H}_{dc} \parallel \mathbf{H}_{ac} \parallel c$). The real, $\mu' = (f/H_0) \int_0^{1/f} B_z(t) \sin(2\pi ft) dt$, and imaginary, $\mu'' = (f/H_0) \int_0^{1/f} B_z(t) \cos(2\pi ft) dt$, fundamental permeabilities are measured by means of two lock-in amplifiers. Our measurements were performed as a function of the temperature (isofield measurements), and also as a function of the applied field (isothermal measurements). In addition, we performed local Hall dc magnetization measurements in order to investigate and clarify the physical mechanisms of the observed hysteretic behavior. Local dc magnetization measurements were performed by applying an ac current ($f = 10$ Hz) to the Hall sensor, and recovering the dc Hall voltage, due to the dc field, by means of a lock-in amplifier. The temperature stabilization was better than 20 mK.

Figure 1 shows the variation of the real part of the local ac permeability $\mu'(H)$ as a function of the applied dc field ($H_{dc} < 1000$ Oe) for various temperatures and ac fields. The measurement at $T = 79.7$ K shows all the characteristic features for the first and second peaks which are present at the

isothermal global magnetization loops. Initially, $\mu'(H)$ displays a small value due to the finite size of the Hall sensor and its nonzero distance from the crystal center. At a particular dc magnetic field, which corresponds to the so-called first peak field H_{fp} , the $\mu'(H)$ starts to increase toward the unit value, which corresponds to the normal state. Subsequently, $\mu'(H)$ increases toward $\mu'(H) = 1$, but then starts to decrease again, forming a local minimum at H_{sp} which obviously corresponds to the second peak, as our local and global dc magnetization measurements affirmed [see Fig. 5(e) below].²⁵ In the higher-temperature regime, in addition to the second peak, a local minimum is formed below the irreversibility point [see Figs. 1(b)–1(d)]. We call this feature the third peak (referring to a peak in the screening current). This behavior was recently observed in other high- T_c superconductors.^{19–25} In measurements at higher temperatures the height of the local minimum which corresponds to the second peak is reduced, and finally, for $T > 86$ K, we were not able to detect it. Contrary to this behavior, the third peak is still evident as we move up to the critical temperature.

Above the irreversibility field H_{irr} , the diamagnetic capability of the superconductor becomes zero, and all the $\mu'(H)$ curves take the value 1. An important information revealed in those measurements is that, in the region between the second peak's end point and the third peak's onset, the response is *almost linear on the amplitude of the applied ac field*, very close to the normal-state value; $\mu'(H) = 1$. This indicates that in this region the vortex system is in a state of very low pinning capability, resulting in an almost negligible screening current.

In order to fix the previous experimental observations, in Fig. 2 we plot the (H, T) phase diagram close to T_c , according to our local isofield and isothermal ac permeability measurements for the $\text{HgBa}_2\text{CuO}_{4+\delta}$ crystal. Depicted are the curves formed by the onset of the second peak, by the second peak points, the end points of the second peak [coming from isothermal $\mu'(H)$ and isofield $\mu'(T)$ measurements], the third peak, and the irreversibility points. In the shaded area between the onset and the second peak lines, a hysteretic behavior is observed. The points of the second peak's onset may mark the boundary between the Bragg glass and the disordered glassy state (*vide infra*).

Figure 3(a) depicts the variation of $\mu'(H)$ as a function of ascending and descending dc magnetic field at various temperatures. Although, in general, the decreasing branch (dashed line) coincides with the increasing one (solid line), we observed a pronounced hysteresis in the regime between the onset H_{onset} and the second peak H_{sp} . In Fig. 3(b) we plot the divergence $\mu'(\text{up}) - \mu'(\text{down})$ of the data of Fig. 3(a) in order to show clearly the hysteretic behavior. We note that the hysteretic peak moves to lower fields for higher temperatures. We observe that hysteresis is more apparent for lower temperatures, as is evident from the reduction of the hysteretic peak as we move to higher temperatures [see Fig. 3(b)]. As we approach the temperature $T = 86$ K, where the second peak line ends, the hysteresis is reduced. In Fig. 3(c) we observe that, at a constant temperature $T = 82$ K, the effect is more pronounced for small ac fields. As we apply higher

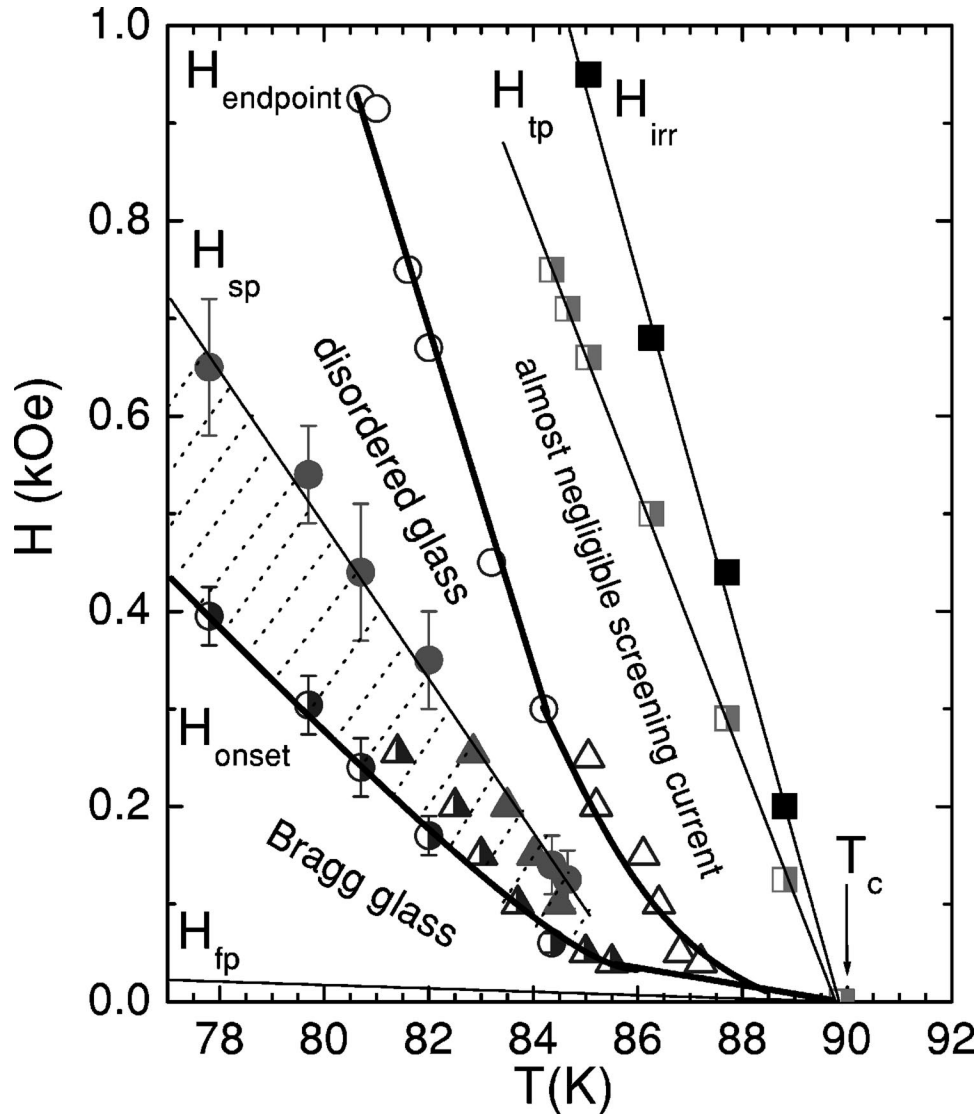


FIG. 2. The phase diagram of vortex matter close to the critical temperature. Presented are the onset of the second peak (semi filled points), the second peak (full points), and the second peak's end point (empty points). Circles come from isothermal $\mu'(H)$ measurements and triangles come from isofield $\mu'(T)$ measurements. In addition we present the third peak (semifilled squares) and the irreversibility points (full squares). The line H_{sp} ends at $T \approx 86$ K, while the H_{onset} and $H_{end\ point}$ lines (thick lines) tend to the critical temperature. The lines are just guides to the eye.

amplitudes the effect is no longer evident. We observed the same behavior in all the temperature regime, up to the end point $T = 86$ K.

The effect of an applied ac perturbation on the hysteretic behavior, observed in some cases in magnetic or transport measurements in high- T_c superconductors, is a subject of intensive interest.^{15,18,40-43} For small ac fields or small transport currents, the driving force acting on vortices is small, so it may be considered as a small perturbation. In this case, thermodynamic or dynamic effects, characterizing a phase transition, may be retained (such as hysteresis or a sudden drop in the resistance observed, for example, at the melting transition of the vortex lattice).^{44,45,42} On the other hand, measurements realized under high transport currents or high ac fields obscure the hysteretic characteristics of a possible underlying phase transition,^{43,42,18} or may dynamically rear-

range a disordered solid state to a more ordered one.^{15,41,40} This is exactly the behavior observed in our measurements. For temperatures close to the end point ($T = 86$ K) of the second peak line, we were not able to observe a hysteretic behavior even for the smallest ac field we could apply.

We must note that such small differences can be detected only with a sensitive local technique, like the one employed in the present work. Local magnetic induction measurements by means of microscopic Hall sensors is a valuable method, because, due to the small size of the active area of the sensor, the filling factor is unity. So one can measure, with high sensitivity, small local changes of the magnetic induction at the surface of small crystals. In addition, the achieved high sensitivity (0.01 Oe) permits us to measure small screening currents such as 10 A/cm² or less. Thereby, we can estimate with high accuracy, from the onset of diamagnetic behavior,

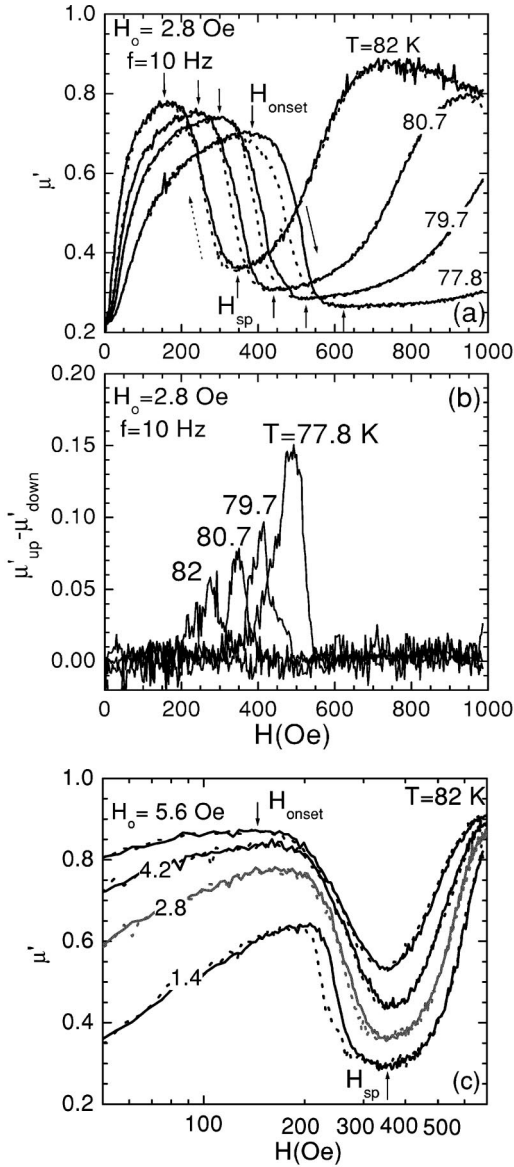


FIG. 3. Real part $\mu' = B'/H_0$ of the local fundamental ac permeability as a function of the dc field (a) at constant $H_0 = 2.8$ Oe and various temperatures $T = 77.8, 79.7, 80.7,$ and 82 K, and (c) at constant temperature $T = 82$ K for various ac fields, $H_0 = 1.4, 2.8, 4.2,$ and 5.6 Oe ($\mathbf{H}_{dc}, \mathbf{H}_{ac} \parallel c$). The solid (dashed) lines correspond to the increasing (decreasing) branch. (b) The divergence $\mu'(\text{up}) - \mu'(\text{down})$ of the increasing and decreasing branches for various temperatures is presented.

the irreversibility line or the transition from one vortex state to another.

Let us now discuss the possible influence of the surface/geometrical barriers in our measurements, in order to show that the observed hysteretic behavior is directly related to a bulk pinning property of vortex matter. For the case of a strong nonlinear current–electric-field $[E(J)]$ relation in the glass regime, one expects a symmetric hysteresis loop of the global or local irreversible dc magnetization (the screening current does not display hysteresis). In such a case, the fundamental permeability is expected to be independent of the measuring path, while descending or ascending the external

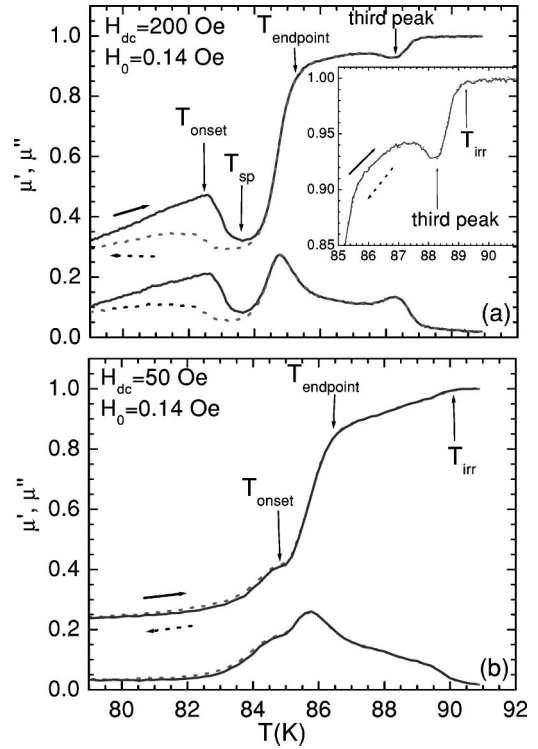


FIG. 4. Temperature variation of the real, μ' , and imaginary, μ'' , parts of the local permeability, for $H_{dc} = 50$ 200 Oe and $H_0 = 0.14$ Oe, for warming (solid lines) above T_c and subsequent cooling (dashed lines) of the vortex system.

magnetic field, in an isothermal measurement. In contrast, for an asymmetric loop of the irreversible dc magnetization, hysteresis in the screening current and the fundamental permeability should also be observed during increases and decreases of the dc field. The presence of surface/geometrical barriers generates an asymmetry in the magnetization loop. This asymmetry is present in an extensive field range. This means that $\mu'(H)$ is expected to display hysteresis in all ranges of the loop measurement. In our case we may rule out the influence of surface/geometrical barriers, because the isothermal variation of $\mu'(H)$ displays a hysteretic behavior only in a particular interval of the applied dc field. *This interval is strictly located in the region between the onset point and the second magnetization peak.*

Another important point revealed in our measurements is that, in the regime where hysteresis is observed, the decreasing branch is placed below the increasing one. This means that the high-field state of vortex matter possesses more diamagnetic capability (higher critical current, J_c) than the low-field state (zero-field cooling initial condition). In the framework of the collective pinning theory,⁴⁶ the critical current is related to the characteristic correlation volume V_c , over which the vortex solid is ordered, via the relation $J_c \propto V_c^{-1/2}$. We see that for a more ordered state (higher collective pinning volume) we have a reduced value for the critical current. The fact that the high-field vortex state exhibits a higher critical current indicates that it is more disordered than the low-field one.

A pronounced hysteretic behavior could also be observed

in isofield ac permeability measurements as a function of the temperature. Figure 4 shows $\mu'(T)$, and $\mu''(T)$ curves for $H_0=0.14$ Oe and $H_{dc}=50$ and 200 Oe. The onset point H_{onset} and the second peak point H_{sp} are placed at higher temperatures for the increasing branch than for the decreasing one. In the inset we present the third peak observed just below the irreversibility point. For high applied ac fields a hysteretic behavior could not be observed, in agreement to the isothermal $\mu'(H)$, $\mu''(H)$ measurements presented above.

At this point we must note that, in measurements realized under very low dc magnetic fields, the characteristic fingerprint of the fishtail peak is not observed even if we change the applied ac field for three orders of magnitude ($0.01 < H_0 < 20$ Oe). Instead, only a sudden drop in the $\mu'(T)$ curves is observed, as is evident for the case of $H_{dc}=50$ Oe. Thus the line H_{sp} , related to the second peak effect, ends at this characteristic point, but the H_{onset} and $H_{end\ point}$ lines tend toward the critical temperature (see Fig. 2).

Is worth noting that the appearance of hysteresis in dynamical measurements may be indicative of a possible underlying transition, but is not necessarily evidence of a phase transition of first order.^{47,48} In order to understand the physical mechanisms associated with the observed hysteresis, we performed partial loop measurements. If the observed hysteresis is directly related to a first-order transition, one would expect that partial hysteresis subloops would also be present, due to the finite latent heat and the different relaxation rates of the two distinct phases.^{47,48} Figure 5 presents partial loop ac permeability measurements for an ac field $H_0=4.2$ Oe at $T=77.8$ K. In the upper and lower panels we present the in-phase and out-of phase local ac magnetic induction signals respectively. At this measurement the procedure is as follows: starting from a field above the peak point we perform minor loops by progressively lowering the minimum value H_{min} of the applied dc field. Remarkably, the minor loops do not follow the complete envelope loop. We observe that the increasing branch of each minor loop (corresponding to a lower value of the minimum applied dc field H_{min}) is placed below the corresponding branch for the next value of H_{min} . At the end, around the onset of the second peak, no hysteretic behavior can be observed. We clearly see that the partial subloops follow exactly the shape of the complete loop, without retracing the same curve after reversing the field sweep. This is a direct characteristic of a first-order transition. In such a case, we expect that every fraction of the vortex solid, which transforms in every partial process, should follow the same thermomagnetic pattern of the complete transition, as in the case where the whole vortex system transforms from one state to another.^{47,49} In addition, the observed thermomagnetic history dependence of the ac response is not compatible to the conventional critical-state model. This model treats the critical current J_c as a single-valued function of the magnetic induction B and temperature T , while our measurements indicate that J_c depends on the measuring path in the regime between H_{onset} and H_{sp} . The observed behavior can be understood as follows: as we expose the system to a lower value of the applied dc field, H_{min}

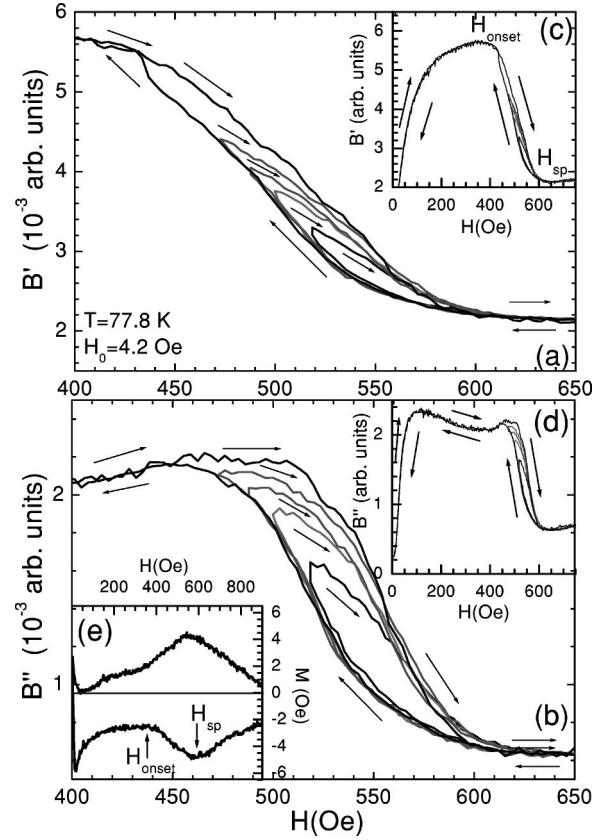


FIG. 5. Partial loop measurements of the real, μ' , and imaginary, μ'' , parts of the local fundamental ac permeability as a function of dc field for $H_0=4.2$ Oe at $T=77.8$ K ($\mathbf{H}_{dc}, \mathbf{H}_{ac} \parallel c$). In the regime between the second peak and its onset point, pronounced thermomagnetic history-dependent effects are observed. Insets: In insets (c) and (d) we present measurements in the whole range. In inset (e) we present a local dc magnetization loop in order to affirm the results of our ac measurements.

the topological defects remaining in the vortex solid decrease, so that the critical current is reduced and the corresponding losses, reflected at the out of phase signal, increase. Since in the elastic theory, the critical current J_c is a single-valued function of B and T , the hardening effects, such as observed in our measurements, could only be ascribed to *plastic deformations in the vortex solid*. This is in agreement to the behavior observed in Refs. 26–29 and 34–37. In insets (c) and (d), we present the complete B'_z (upper panel) and B''_z (lower panel) curves, while in inset (e) we present the local dc magnetization loop at $T=77.8$ K, in order to consolidate our experimental results.

Finally, we would like to discuss what happens at the region where the fishtail peak is terminated. First we recall that, although the line H_{sp} ends at a characteristic point (86 K and 50 Oe), at higher temperatures we observed a sudden drop in our $\mu'(T)$ curves [see Fig. 4(b)]. So, the two related lines, referring to the onset and the end points of this sudden drop [see Fig. 4(b)], seem to continue all the way up to the critical temperature [see Fig. 2]. Placing beyond dispute that the onset line, H_{onset} separates a Bragg glass phase from a totally disordered glass, we discuss a possible interpretation

of the behavior observed in the regime of the phase diagram close to the irreversibility line H_{irr} . Our local ac permeability measurements, as a function of dc magnetic field, imply that in the region between the second peak's end point and the third peak's onset, the screening current is almost negligible, as already discussed above. In addition, the measured response $\mu'(H)$ in this regime is almost linear on the amplitude of the ac field [see Figs. 1(b) and 1(c)]. Taking into account the above experimental observations, we propose that at the end point line, $H_{end\ point}$, the disordered glass transforms to another phase. A candidate vortex phase, exhibiting such a characteristic behavior ($J_c \sim 0$), could be a viscous *liquid state* of flux lines. This phase, as we raise the temperature or dc field, transforms, at the irreversibility point H_{irr} , to a *gas state* of pancake vortices.^{50,51,25} On the other hand, the disordered glass could extend in the whole regime up to the irreversibility line, H_{irr} , and the end point line $H_{end\ point}$ represents a simple boundary where only the dynamic behavior is changed. Above the line $H_{end\ point}$ the solid glass is weakly pinned, probably due to the fact that the depinning temperature is exceeded. As we farther raise the temperature (or dc field), the disordered glass melts, by exhibiting an additional peak in the screening current (third peak). This point of view is consistent with recent numerical

simulations, revealing that the screening current exhibits a peak, both across the Bragg glass to vortex glass transition (fishtail peak or second peak effect) and across the melting line (peak effect or third peak).⁵²

In summary, we presented local Hall ac permeability measurements as a function of the applied dc field (isothermal) and temperature (isofield) for a $\text{HgBa}_2\text{CuO}_{4+\delta}$ single crystal with $T_c = 89.9$ K. The second peak line ends a few K below the critical temperature. At the onset of the second peak we observed a pronounced hysteretic behavior and thermomagnetic history effects, giving evidence of a possible underlying first-order phase transition between an almost ordered lattice state, where elastic behavior dominates, and a disordered glassy state, where plastic deformations are more important. Recently, experimental evidence was provided of a first-order transition between the Bragg glass and the disordered phase in $\text{Bi}_2\text{Sr}_2\text{CaCu}_2\text{O}_{8+\delta}$ and 2H-NbSe_2 single crystals.⁵³⁻⁵⁷ We hope that our results will assist in the investigation of the nature of the order-disorder transition.

This work was supported by the Greek Secretariat for Research and Technology through the PENED program (99ED186) and Dimoerevna program (642).

-
- ¹G. Blatter, M.V. Feigel'man, V.B. Geshkenbein, A.I. Larkin, and V.M. Vinokur, *Rev. Mod. Phys.* **66**, 1125 (1994).
²E.H. Brandt, *Rep. Prog. Phys.* **58**, 1465 (1995).
³M.P.A. Fisher, *Phys. Rev. Lett.* **62**, 1415 (1989); D.S. Fisher, M.P.A. Fisher, and D.A. Huse, *Phys. Rev. B* **43**, 130 (1991).
⁴T. Giamarchi and P. Le Doussal, *Phys. Rev. B* **52**, 1242 (1995); **55**, 6577 (1997); *Phys. Rev. Lett.* **72**, 1530 (1994).
⁵D. Ertas and D.R. Nelson, *Physica C* **272**, 79 (1996).
⁶M.J.P. Gingras and D.A. Huse, *Phys. Rev. B* **53**, 15193 (1996).
⁷A.E. Koshelev and V.M. Vinokur, *Phys. Rev. B* **57**, 8026 (1998).
⁸V. Vinokur, B. Khaykovich, E. Zeldov, M. Konczykowski, R.A. Doyle, and P.H. Kes, *Physica C* **295**, 209 (1998).
⁹J. Kierfield, *Physica C* **300**, 171 (1998).
¹⁰J. Kierfield and V. Vinokur, *Phys. Rev. B* **61**, R14 928 (2000); *Phys. Rev. Lett.* **85**, 4948 (2000).
¹¹G.P. Mikitik and E.H. Brandt, *Phys. Rev. B* **64**, 184514 (2001).
¹²T. Klein, I. Journaud, S. Blanchard, J. Marcus, R. Cubbit, T. Giamarchi, and P. Le Doussal, *Nature (London)* **413**, 404 (2001).
¹³R. Wordenweber, P.H. Kes, and C.C. Tsuei, *Phys. Rev. B* **33**, 3172 (1986).
¹⁴G. Ravikumar, V.C. Sahni, P.K. Mishra, T.V.C. Rao, S.S. Banerjee, A.K. Grover, S. Ramakrishnan, S. Bhattacharya, M.J. Higgins, E. Yamamoto, Y. Haga, M. Hedo, Y. Inada, and Y. Onuki, *Phys. Rev. B* **57**, R11 069 (1998).
¹⁵W. Henderson, E.Y. Andrei, and M.J. Higgins, *Phys. Rev. Lett.* **81**, 2352 (1998); W. Henderson, E.Y. Andrei, M.J. Higgins, and S. Bhattacharya, *ibid.* **77**, 2077 (1996).
¹⁶S. Bhattacharya and M.J. Higgins, *Phys. Rev. B* **52**, 64 (1995).
¹⁷A.C. Marley, M.J. Higgins, and S. Bhattacharya, *Phys. Rev. Lett.* **74**, 3029 (1995).
¹⁸X.S. Ling, J.E. Berger, and D.E. Proper, *Phys. Rev. B* **57**, 3249 (1998).
¹⁹A.A. Zhukov, H. Kupfer, G. Perkins, L.F. Cohen, A.D. Caplin, S.A. Klestov, H. Claus, V.I. Voronkova, T. Wolf, and H. Wuhl, *Phys. Rev. B* **51**, 12 704 (1995).
²⁰K. Deligiannis, P.A.J. de Groot, M. Oussena, S. Pinfold, R. Langan, R. Gagnon, and L. Taillefer, *Phys. Rev. Lett.* **79**, 2121 (1997).
²¹A.I. Rykov, S. Tajima, F.V. Kusmartsev, E.M. Forgan, and Ch. Simon, *Phys. Rev. B* **60**, 7601 (1999).
²²A. Zhukov, P.A.J. de Groot, S. Kokkaliaris, E. di Nicolò, A.G.M. Jansen, E. Mossang, G. Martinez, P. Wyder, T. Wolf, H. Kupfer, H. Asaoka, R. Gagnon, and L. Taillefer, *Phys. Rev. Lett.* **87**, 017006 (2001).
²³D. Pal, S. Ramakrishnan, A.K. Grover, D. Dasgupta, and B.K. Sarma, *Phys. Rev. B* **63**, 132505 (2001).
²⁴S. Sarkar, D. Pal, P.L. Paulose, S. Ramakrishnan, A.K. Grover, C.V. Tomy, D. Dasgupta, B.K. Sarma, G. Balakrishnan, and D. McK. Paul, *Phys. Rev. B* **64**, 144510 (2001).
²⁵D. Stamopoulos and M. Pissas, *Supercond. Sci. Technol.* **14**, 844 (2001).
²⁶B. Janossy, L. Nguyen, and P. Wyder, *Phys. Rev. B* **53**, 11 845 (1996).
²⁷H. Kupfer, S.N. Gordeev, W. Jahn, R. Kresse, R. Meier-Hirmer, T. Wolf, A.A. Zhukov, K. Salama, and D. Lee, *Phys. Rev. B* **50**, 7016 (1994).
²⁸Y. Abulafia, A. Shaulov, Y. Wolfus, R. Prozorov, L. Burlachkov, Y. Yeshurun, D. Majer, E. Zeldov, H. Wuhl, V.B. Geshkenbein, and V.M. Vinokur, *Phys. Rev. Lett.* **77**, 1596 (1996).
²⁹M. Pissas, D. Stamopoulos, E. Moraitakis, G. Kallias, D. Niarchos, and M. Charalambous, *Phys. Rev. B* **59**, 12 121

- (1999); D. Stamopoulos, M. Pissas, E. Moraitakis, G. Kallias, D. Niarchos, and M. Charalambous, *Physica C* **317**, 658 (1999).
- ³⁰T. Nishizaki, T. Naito, and N. Kobayashi, *Phys. Rev. B* **58**, 11 169 (1998).
- ³¹B. Khaykovich, E. Zeldov, D. Majer, T.W. Li, P.H. Kes, and M. Konczykowski, *Phys. Rev. Lett.* **76**, 2555 (1996).
- ³²B. Khaykovich, M. Konczykowski, E. Zeldov, R.A. Doyle, D. Majer, P.H. Kes, and T.W. Li, *Phys. Rev. B* **56**, R517 (1997).
- ³³D. Giller, A. Shaulov, Y. Yeshurun, and J. Giapintzakis, *Phys. Rev. B* **60**, 106 (1999).
- ³⁴Y. Radzyner, S.B. Roy, D. Giller, Y. Wolfus, A. Shaulov, P. Chad-dah, and Y. Yeshurun, *Phys. Rev. B* **61**, 14 362 (2000).
- ³⁵M. Pissas, E. Moraitakis, G. Kallias, and A. Bondarenko, *Phys. Rev. B* **62**, 1446 (2000).
- ³⁶S. Kokkaliaris, P.A.J. de Groot, S.N. Gordeev, A.A. Zhukov, R. Gagnon, and L. Taillefer, *Phys. Rev. Lett.* **82**, 5116 (1999).
- ³⁷S. Kokkaliaris, A.A. Zhukov, P.A.J. de Groot, R. Gagnon, L. Taillefer, and T. Wolf, *Phys. Rev. B* **61**, 3655 (2000).
- ³⁸M. Pissas, B. Billon, M. Charalambous, J. Chaussy, S. LeFloch, P. Bordet, and J.J. Caponi, *Supercond. Sci. Technol.* **10**, 598 (1997).
- ³⁹M. Pissas, E. Moraitakis, G. Kallias, A. Terzis, D. Niarchos, and M. Charalambous, *Phys. Rev. B* **58**, 9536 (1998).
- ⁴⁰S.O. Valenzuela and V. Bekeris, *Phys. Rev. Lett.* **84**, 4200 (2000); **86**, 504 (2001).
- ⁴¹F. Pardo, F. De La Cruz, P.L. Gammel, C.S. Oglesby, E. Bucher, B. Batlogg, and D.J. Bishop, *Phys. Rev. Lett.* **78**, 4633 (1997).
- ⁴²J.A. Fendrich, U. Welp, W.K. Kwok, A.E. Koshelev, G.W. Crabtree, and B.W. Veal, *Phys. Rev. Lett.* **77**, 2073 (1996); G.W. Crabtree, W.K. Kwok, U. Welp, J.A. Fendrich, and B.W. Veal, *J. Low Temp. Phys.* **105**, 1073 (1996).
- ⁴³W.K. Kwok, S. Fleshler, U. Welp, V.M. Vinokur, J. Downey, G.W. Crabtree, and M.M. Miller, *Phys. Rev. Lett.* **69**, 3370 (1992); W.K. Kwok, J. Fendrich, U. Welp, S. Fleshler, J. Downey, and G.W. Crabtree, *ibid.* **72**, 1088 (1994).
- ⁴⁴M. Charalambous, J. Chaussy, and P. Lejay, *Phys. Rev. B* **45**, 5091 (1992); M. Charalambous, J. Chaussy, P. Lejay, and V. Vinokur, *Phys. Rev. Lett.* **71**, 436 (1993).
- ⁴⁵H. Safar, P.L. Gammel, D.A. Huse, D.J. Bishop, J.P. Rice, and D.M. Ginsberg, *Phys. Rev. Lett.* **69**, 824 (1992).
- ⁴⁶A. Larkin and Y. Ovchinnikov, *J. Low Temp. Phys.* **34**, 409 (1979).
- ⁴⁷W. Jiang, N.C. Yeh, D.S. Reed, U. Kriplani, and F. Holtzberg, *Phys. Rev. Lett.* **74**, 1438 (1995).
- ⁴⁸V.B. Geshkenbein, L.B. Ioffe, and A.I. Larkin, *Phys. Rev. B* **48**, 9917 (1993).
- ⁴⁹G.W. Crabtree, W.K. Kwok, U. Welp, J.A. Fendrich, and B.W. Veal, *J. Low Temp. Phys.* **105**, 1073 (1996).
- ⁵⁰L.I. Glazman and A.E. Koshelev, *Phys. Rev. B* **43**, 2835 (1991).
- ⁵¹G. Blatter, V. Geshkenbein, A. Larkin, and H. Nordborg, *Phys. Rev. B* **54**, 72 (1996).
- ⁵²A. van Otterlo, R.T. Scalettar, G.T. Zimnyi, R. Olsson, A. Petrean, W. Kwok, and V. Vinokur, *Phys. Rev. Lett.* **84**, 2493 (2000).
- ⁵³C.J. van der Beek, S. Colson, M.V. Indenbom, and M. Konczykowski, *Phys. Rev. Lett.* **84**, 4196 (2000).
- ⁵⁴D. Giller, A. Shaulov, T. Tamegai, and Y. Yeshurun, *Phys. Rev. Lett.* **84**, 3698 (2000).
- ⁵⁵M.B. Gaifullin, Yuji Matsuda, N. Chikumoto, J. Shimoyama, and K. Kishio, *Phys. Rev. Lett.* **84**, 2945 (2000).
- ⁵⁶N. Avraham, B. Khaykovich, Y. Myasoedov, M. Rappaport, H. Shtrikman, Dima E. Feldman, T. Tamegai, P.H. Kes, M. Lik, M. Konczykowski, K.J. van der Beek, and E. Zeldov, *Nature (London)* **411**, 451 (2001).
- ⁵⁷Y. Paltiel, E. Zeldov, Y. Myasoedov, M.L. Rappaport, G. Jung, S. Bhattacharya, M.J. Higgins, Z.L. Xiao, E.L. Xiao, E.Y. Andrei, P.L. Gammel, and D.J. Bishop, *Phys. Rev. Lett.* **85**, 3712 (2000).